JNeurosci
THE JOURNAL OF NEUROSCIENCE

Research Articles: Behavioral/Cognitive

Moment-to-moment BOLD Signal Variability Reflects Regional Changes in Neural Flexibility Across the Lifespan

Jason S. Nomi[a], Taylor S. Bolt[a], Chiemeka Ezie, Lucina Q. Uddin[a,b] and Aaron S. Heller[a,b,c]

[a]*Department of Psychology, University of Miami, Coral Gables, FL, USA 33124*
[b]*Neuroscience Program, University of Miami Miller School of Medicine, Miami, FL, USA 33136*
[c]*Department of Psychiatry, University of Miami, Miami, FL, USA 33136*

DOI: 10.1523/JNEUROSCI.3408-16.2017

Received: 3 November 2016

Revised: 24 April 2017

Accepted: 26 April 2017

Published: 3 May 2017

Author contributions: J.S.N., L.Q.U., and A.S.H. designed research; J.S.N., T.B., C.E., L.Q.U., and A.S.H. performed research; J.S.N., T.B., and A.S.H. contributed unpublished reagents/analytic tools; J.S.N., T.B., and C.E. analyzed data; J.S.N., L.Q.U., and A.S.H. wrote the paper.

This work was supported by award R01MH107549 from the National Institute of Mental Health, a NARSAD Young Investigator Grant, and a University of Miami Convergence Research Grant to LQU.

Corresponding authors: Jason S. Nomi, Ph.D., Department of Psychology, University of Miami, P.O. Box 248185, Coral Gables, FL 33124, USA, Email: jxn131@miami.edu, Fax: +1 305-284-3402, Phone: +1 305-284-3265, Designed research, performed research, analyzed data, wrote the paper Lucina Q. Uddin, Ph.D., Department of Psychology, University of Miami, P.O. Box 248185, Coral Gables, FL 33124, USA, Email: l.uddin@miami.edu, Fax: +1 305-284-3402, Phone: +1 305-284-3265, Designed research, performed research, wrote the paper

Cite as: J. Neurosci ; 10.1523/JNEUROSCI.3408-16.2017

Moment-to-moment BOLD Signal Variability Reflects Regional Changes in Neural Flexibility Across the Lifespan

Abbreviated Title:

BOLD Signal Variability Changes Across the Lifespan

*Jason S. Nomi[a], Taylor S. Bolt[a], Chiemeka Ezie, *Lucina Q. Uddin[a,b], & Aaron S. Heller[a,b,c]

[a]Department of Psychology, University of Miami, Coral Gables, FL, USA 33124
[b]Neuroscience Program, University of Miami Miller School of Medicine, Miami, FL, USA 33136
[c] Department of Psychiatry, University of Miami, Miami, FL, USA 33136

***Corresponding authors:**

Jason S. Nomi, Ph.D.
Department of Psychology
University of Miami
P.O. Box 248185
Coral Gables, FL 33124, USA
Email: jxn131@miami.edu
Fax: +1 305-284-3402, Phone: +1 305-284-3265
Designed research, performed research, analyzed data, wrote the paper

Taylor S. Bolt, M.S.
Department of Psychology
University of Miami
P.O. Box 248185
Coral Gables, FL 33124, USA
Email: tsb46@miami.edu
Fax: +1 305-284-3402, Phone: +1 305-284-3265
Performed research, analyzed data

Chiemeka Ezie, B.S.
Department of Psychology
University of Miami
P.O. Box 248185
Coral Gables, FL 33124
Email: cezie@miami.edu
Phone: +1 305 284 9555
Performed research, analyzed data

Lucina Q. Uddin, Ph.D.
Department of Psychology
University of Miami
P.O. Box 248185
Coral Gables, FL 33124, USA
Email: l.uddin@miami.edu
Fax: +1 305-284-3402, Phone: +1 305-284-3265
Designed research, performed research, wrote the paper

Aaron S. Heller, Ph.D.
Department of Psychology
University of Miami
P.O. Box 248185
Coral Gables, FL 33124
Email: aheller@miami.edu
Phone: +1 305 284 9498
Designed research, performed research, analyzed data, wrote the paper

Acknowledgments: This work was supported by award R01MH107549 from the National Institute of Mental Health, a NARSAD Young Investigator Grant, and a University of Miami Convergence Research Grant to LQU.

Abstract

Variability of neuronal responses is thought to underlie flexible and optimal brain function. Because previous work investigating BOLD signal variability has been conducted within task-based fMRI contexts on adults and older individuals, very little is currently known regarding regional changes in spontaneous BOLD signal variability in the human brain across the lifespan. The current study utilized resting state fMRI data from a large sample of male and female human participants covering a wide age range (6-85 years) across two different fMRI acquisition parameters (TR = 0.645 and 1.4 seconds). Variability in brain regions including a key node of the salience network (anterior insula) increased linearly across the lifespan across datasets. In contrast, variability in most other large-scale networks decreased linearly over the lifespan. These results demonstrate unique lifespan trajectories of BOLD variability related to specific regions of the brain and add to a growing literature demonstrating the importance of identifying normative trajectories of functional brain maturation.

Significance Statement

Although brain signal variability has traditionally been considered a source of unwanted noise, recent work demonstrates that variability in brain signals during task performance is related to brain maturation in old age as well as individual differences in behavioral performance. The current results demonstrate that intrinsic fluctuations in resting-state variability exhibit unique maturation trajectories in specific brain regions and systems, particularly those supporting salience detection. These results have implications for investigations of brain development and aging, as well as interpretations of brain function underlying behavioral changes across the lifespan.

Introduction

Blood oxygenated level-dependent (BOLD) signal variability is often considered as a source of unwanted noise. This is in contrast to theories proposing that biological variability is necessary for optimal brain function (McIntosh et al., 2010; Garrett et al., 2013; Tognoli and Kelso, 2014). For example, coordination dynamics theory proposes that networks fluctuate between integration, segregation, and metastable configurations (Tognoli and Kelso, 2014). Metastability requires a balance between integration and segregation, where signal variability within a network facilitates shifting between integration and segregation. That is, networks demonstrating high integration or segregation without variability cannot flexibly shift between configurations. On the other hand, networks with high variability can flexibly shift through integrative and segregative configurations. Another approach highlighting the importance of neural variability is the "bayes optimal theory" that proposes if neurons fired identically to stimuli over time, systems would not adapt to that stimulus in different circumstances (Beck et al., 2008). These perspectives posit that variability in neuronal response is a critical component of brain function.

Accumulating research has demonstrated differences in BOLD variability between older adults compared with younger adults in a number of task-based fMRI contexts. BOLD variability in the majority of brain regions decreases during task-based fixation periods (i.e., task-absent) in older adults compared with younger adults (Garrett et al., 2010). Increased BOLD variability has also been linked to younger individuals, with faster reaction time and more consistent performance in perceptual matching and attentional cueing tasks (Garrett et al., 2011). Greater BOLD variability during the fixation period of a task is also associated with more efficient behavioral performance in younger adults compared with older adults (Garrett et al., 2012). Such studies generally demonstrate that BOLD variability decreases across development, with few regions demonstrating increased variability across development. Nonetheless, both increases and decreases in variability have been found throughout frontal, parietal, and temporal brain areas. Additionally, increased left inferior frontal junction variability has been linked to improved performance on a cognitive flexibility task, but impaired performance on an inhibition task (Armbruster-Genç et al., 2016). This suggests that the beneficial impact of regional BOLD variability may be task- and circuit-dependent. Finally, increased variability in the nucleus accumbens has been associated with greater financial risk-taking in older age (Samanez-Larkin et al., 2010). Taken together, these studies demonstrate that greater variability is associated with younger individuals, faster and more consistent performance, and cognitive flexibility, demonstrating its importance as a neural signature of optimal task performance.

The aforementioned studies have mainly examined the effects of BOLD variability within task-based fMRI contexts in younger adults (20-35 years old) and older adults (65-80 years old). However, no studies to date have characterized resting-state BOLD variability nor have they examined variability across the entire lifespan. This is important for two reasons: First, although previous studies analyzed fixation periods within task-based fMRI paradigms, fixation periods are short in duration and may be influenced by task based processing demands (Northoff et al., 2010). Resting-state fMRI offers temporal continuity across the time-series, unaffected by possible task-based influences that could differentially impact individuals at different ages. Second, exploring variability across the lifespan allows for characterization of both linear and quadratic effects. This is important because such effects are present in lifespan resting-state fMRI studies charting functional connectivity trajectories (Betzel et al., 2014; Cao et al., 2014).

To explore these questions, the current study utilized two groups of resting state fMRI data (*n*=187 and *n*=191; 6 - 85 years old) to examine lifespan trajectories of BOLD variability and demonstrate replicability of findings across different multi-band acquisition parameters. Based on predictions from the previous task-based fMRI literature examining fixation periods between task blocks (Garrett et al., 2010), we expected to find that a majority of voxels would demonstrate decreases in variability across the lifespan, and that a minority of voxels would demonstrate increases in variability across the lifespan.

Methods

Participants

Two resting state fMRI datasets (fast TR group: *n* = 191, TR = 0.645s; slow TR group: *n* = 187, TR = 1.4s), each containing ten minutes of data, were downloaded from the NKI-enhanced database (Nooner et al., 2012) (**Figure 1**). The two groups both included participants from a wide age range (6 – 85 years of age) and differed principally in multi-band TR acquisition time. Group one, the “fast TR group” (TR = 0.645 seconds) included 191 participants (132 female; Mean age = 42.26 years old, SD = 23.60; Mean Full scale IQ = 104.31, SD = 14.06; Mean framewise displacement (FD) = 0.12, SD = 0.04). Handedness was assessed using the Edinburgh Handedness Questionnaire (EHQ)(Oldfield, 1971) on a scale of -100 to 100; 19 participants had negative scores. Group two, the “slow TR group” (TR = 1.4 seconds) included 187 participants (131 female; Mean age = 42.46 years old, SD = 23.30; Mean Full scale IQ = 104.54, SD = 13.75; Mean FD = 0.26, SD = 0.12; 20 participants had negative EHQ scores). We included both data sets with different TRs in our analyses to ensure the robustness and reliability of any MSSD effects as a function of age. This procedure mitigates concerns regarding the unknown influence on the reliability of MSSD results from data acquired utilizing recently developed multi-band EPI protocols (Smith et al., 2013).

Inclusion criteria for both data sets were the following: subjects had no current or past DSM diagnosis for psychiatric disorders, and less than 3mm in translational head movement and/or 3 degrees of rotational head movement. There were 177 subjects that appeared in both groups. Subjects appeared in one group but not the other because of increased head motion during one scan, but not the other, or poor/missing functional scans in one dataset or the other. There were no significant differences in age ($t(376) = 0.08$, $p = 0.93$) or in IQ ($t(376) = 0.16$, $p = 0.87$) in the two TR groups, as most subjects contributed data to both groups. However, there was a significant difference in FD ($t(376) = 15.46$, $p = 4.31 \times 10^{-42}$) between the groups. Larger FD for the slow TR group was expected: head movement would be naturally smaller for the fast TR group because there is less time to move between successive volume acquisitions. Because of these differences in head movement between TR groups, and the stringent employment of head motion analysis corrections we employed, we reasoned that any MSSD effects that replicated across both groups would ameliorate concerns that head movement influenced the results.

Imaging was performed on a Siemens Trio 3.0 T scanner that collected a T1 anatomical image and multiband (factor of 4) EPI sequenced resting state images (Low

TR group: 3 x 3 x 3 mm, 40 interleaved slices, TE = 30 ms, flip angle = 60 degrees, field of view = 222 mm, 900 volumes; High TR group: 2 x 2 x 2 mm, 64 interleaved slices, TE = 30 ms, flip angle = 65 degrees, field of view = 224 mm, 404 volumes). Participants were instructed to keep their eyes open and fixate on a central cross in the middle of the screen (http://fcon_1000.projects.nitrc.org/indi/enhanced/mri_protocol.html).

Image Preprocessing

Resting state scans were preprocessed using FSL, AFNI, and SPM 8 functions through DPARSF-A (http://rfmri.org/DPARSF). The first five volumes were removed to allow the data to reach T1 equilibrium. Several steps were undertaken to remove motion artifacts and other sources of noise from the data prior to analysis. Resting state data were realigned (FSL) and smoothed (FSL: 6mm) before individual independent component analyses (ICA) were conducted for all data sets using automatic dimensionality estimation (FSL's MELODIC). Noise components were then classified for 20 subjects in the fast TR group and 20 subjects in the slow TR group (random sampling by choosing subjects separated by approximately 5 years of age) by transforming independent component maps into MNI space (3mm for the fast TR group and 2mm for the slow TR group to match their respective acquisition parameters). The resulting component classifications were then fed into FMIRB's ICA-FIX classification algorithm (Griffanti et al., 2014). ICA-FIX to classify noise and non-noise components from both groups before conducting nuisance regression of classified noise components from the resting state scans in subject space. The ICA-FIX cleaned data was then normalized into MNI space (DPARSF-A) using an EPI template from SPM (3 mm for the low TR group and 2 mm for the high TR group to match each group's respective acquisition parameters). The data were then despiked using AFNI's 3dDespike algorithm, subjected to nuisance covariance regression (Friston 24 motion parameters, WM, CSF), linear detrended, and band-pass filtered (0.01 - 0.10 Hz) to isolate low frequency fluctuations that characterize resting-state BOLD signals (Damoiseaux et al., 2006).

Experimental Design and Statistical Analysis

The current study examined the relationship between bold variability and age using a voxel-wise within-subjects measure called mean square successive difference (MSSD). MSSD was calculated on a voxel-wise basis for all subjects using custom Matlab scripts. For more details, see the methods section, "BOLD Signal Variability".

The voxel-wise relationship between MSSD and age was tested using an ordinary least squares (OLS) regression model in FSL using a repeated measures design with linear age, quadratic age as regressors of interest, and handedness, FD, IQ as nuisance regressors. In order to account for multiple voxel-wise comparisons, spatial maps from the OLS analysis were subjected to a voxel-wise threshold of $p < 0.002$ (uncorrected) and a cluster-wise threshold of $p < 0.5$ (corrected using Gaussian Random Field Theory; GRF). For more details on the OLS analysis, see the methods section, "BOLD Signal Variability".

Post-hoc testing of significant cluster corrected effects using a linear regression analysis in SPSS 24 was conducted in order to further examine linear and quadratic effects identified from the OLS analysis. This was done to ensure that significant effects identified from the voxel-wise analysis remained significant when averaging MSSD across a number of voxels, and to account for possible influences of gray matter probability and gender. For more details, see the methods section, "Post-hoc Analysis of Gray Matter Probability, Gender, Linear, and Quadratic Effects".

Additional post-hoc testing consisted of examining the relationship between MSSD values for only the 177 subjects present in both TR groups. Spearman's rank order correlations were conducted in SPSS 24 on the effects examined in the previously described post-hoc regression analyses. For more details, see the results section, "Linear relationship between MSSD values for subjects in both TR groups".

BOLD Signal Variability Analysis

Preprocessed time series were converted to z statistics (zero mean, unit standard deviation) before calculating MSSD scores for each voxel (Von Neumann et al., 1941). MSSD was utilized in the current study because of the temporal continuity afforded by resting state data and because it avoids the influence of auto-correlation that is exacerbated by multi-band EPI acquisition parameters (Smith et al., 2013), on measures such as the standard deviation (Arbabshirani et al., 2014). MSSD was calculated by subtracting time point t from time point t + 1, squaring the result, then averaging all resulting values acquired from the entire voxel time course.

$$\delta^2 = \frac{\sum_{i=1}^{n-1}(x_{i+1} - x_i)^2}{n-1}$$

Associations between MSSD and age were calculated in FSL using ordinary least squares regression (OLS). Age regressors included the linear (mean centered) and quadratic age (squared mean centered age). Full-scale IQ, EHQ handedness scores, and FD were included as nuisance regressors. The resulting t-maps were first examined using a liberal voxel-wise correction (uncorrected $p < 0.40$) without cluster size correction.

These more general results demonstrated the reliability of the effects across the two different acquisition times (see **Figure 1**).

T-maps were then examined by employing stricter voxel wise (uncorrected at $p < 0.002$ for linear effects and at $p < 0.05$ for quadratic effects; see results for additional details) and cluster size (corrected at $p < 0.05$) correction to identify results less susceptible to type 1 errors (Eklund et al., 2016). Spatial maps identifying brain areas with significant overlapping effects across both TR groups were produced to further isolate replicable effects. Overlapping effects across TR groups were identified by resampling the slow TR group results to have the same voxel resolution as the fast TR group results (down-sampling the slow TR group cluster-corrected spatial t-maps to $3mm^3$). We then overlaid the fast TR group cluster-corrected results on corresponding cluster-corrected maps for the slow TR group to identify cluster-corrected effects present in both TR groups. MSSD values from each TR group for overlapping significant cluster corrected voxels were then extracted and converted to z statistics to create scatterplots for visualization of lifespan trajectories.

Post-hoc Analysis of Gray Matter Probability, Gender, Linear, and Quadratic Effects

Three regression analyses were run in order to rule out the influence of gray matter probability (GMP) and gender and also to further explore linear and quadratic voxel-wise effects. The primary goal of these follow-up tests was to account for differences in gray matter and gender, and to confirm that voxel-wise effects persisted when averaging MSSD across a group of voxels. Following previous work accounting for changes in gray matter (Damoiseaux et al., 2008), we used ROIs of the overlapping cluster-corrected results from the previous voxel-wise analysis to calculate individual subject estimates of GMP. GMP and gender were then used in subsequent analyses as nuisance regressors. GMP was assessed by segmenting the T1 structural images into gray matter, white matter, and cerebral spinal fluid probability maps in SPM and taking the mean GMP in the ROI. A secondary goal of further exploring linear and quadratic effects was also carried out through these three post-hoc regression analyses.

Three post-hoc regression models were run. The first post-hoc regression model tested whether the MSSD linear effects indeed extend across the lifespan without the quadratic predictor in the model, and to confirm that these linear effects persisted when accounting for GMP and gender. As with previous regression tests, this model utilized linear age (mean centered) as a regressor of interest along with handedness, IQ, FD, GMP, and gender as nuisance covariates. This model was run on ROIs representing significant group-overlapping linear effects from the cluster-corrected voxel-wise analysis.

A second post-hoc regression model was used to test whether a quadratic effect better explained the MSSD trajectory than the linear effect from the first regression model. This model utilized linear age (mean centered) and quadratic age (squared mean centered age) as regressors of interest along with handedness, IQ, FD, GMP, and gender as nuisance covariates. As with the first model, this model was run solely on ROIs representing significant group-overlapping linear effects from the cluster-corrected voxel-wise analysis. We determined that a quadratic model was a better fit compared to the linear model if the quadratic term was statistically significant ($p < 0.05$).

Finally, a third post-hoc regression model was used to confirm that voxel-wise quadratic effects persisted when controlling for GMP and gender. This model utilized linear age (mean centered) and quadratic age (squared mean centered age) as regressors of interest along with handedness, IQ, FD, GMP, and gender as nuisance covariates. This model was run on ROIs representing group-overlapping quadratic effects from the voxel-wise analysis.

Results

Associations between MSSD and Linear Effects of Age

The average whole-brain MSSD value across all subjects was 0.0451 (SD = 0.004, range across subjects: 0.0336 – 0.0561) for the fast TR group and 0.2063 (SD = 0.0175, range across subjects: 0.1625 – 0.2485) for the slow TR group indicating significantly smaller MSSD for the fast TR group ($t(376) = 124.17$, $p = 2.7035 \times 10^{-307}$). This mirrored differences in head motion metrics across TR groups and was also expected, as there should be less difference between the BOLD signal for consecutive volumes when they are acquired closer together in time. Thus, any effects replicating across both TR groups should not be due to the absolute size of MSSD, but rather are due to the contrasts of interest.

Previous research has demonstrated that MSSD and standard deviation (SD) are strongly correlated (*r*'s > 0.97) within the context of a task-based fMRI study (Garrett et al., 2011). In order to examine how MSSD and SD are related in the context of a resting-state fMRI study, voxel-wise estimates of SD were calculated on non-normalized time-courses for all gray-matter voxels. Average correlations between MSSD and SD for gray matter voxels across the whole-brain were then calculated across all subjects in each TR group. Strong positive correlations were present for both the fast (mean $r = 0.73$, SD =

0.037) and slow (mean $r = 0.72$, SD = 0.046) TR groups replicating previous findings of strong correspondence between MSSD and SD.

General linear age MSSD effects revealed both increases and decreases in functionally distinct cortical and subcortical brain areas. Spatial maps for each TR group with a liberal voxel-wise criteria ($p < 0.40$) and no cluster size correction **(Figure 2)** demonstrate that MSSD increases linearly across the lifespan in salience network (SN) nodes (bilateral anterior insula) and bilateral ventral temporal cortices. Linear decreases in MSSD as a function of age appear in the thalamus and basal ganglia and brain networks representing visual, sensorimotor, central executive network (CEN), and nodes of the default mode network (DMN). These results demonstrate that an intrinsic brain pattern of BOLD variability related to maturation across the lifespan is characterized by an increase in SN and ventral temporal cortex (VTC) variability and a decrease in variability for most every other brain area including nodes in the CEN, and DMN along with brain areas in visual, sensorimotor, and subcortical areas. These general results were replicated across both TRs, providing evidence for the robustness of the observed effects.

Spatial maps (**Figure 3)** and scatter plots (**Figure 4**) are presented from brain regions where there was a significant cluster-corrected association with age in both TR groups. This included a linear MSSD increase across the lifespan in the right dorsal anterior insula (dAI) and left VTC. This also included a linear MSSD decrease across the lifespan in bilateral visual and sensorimotor networks, as well as bilateral thalamus and basal ganglia regions.

Associations between MSSD and Nonlinear Effects of Age

There were no quadratic effects of age that survived cluster correction at the stringent criterion of voxel-wise ($p < 0.002$, Fast TR group $df = 189$, Slow TR group $df = 185$) and cluster wise ($p < 0.05$). There were two quadratic effects that survived a more liberal correction of voxel-wise ($p < 0.05$ and cluster wise ($p < 0.05$). Although these effects in isolation are more susceptible to Type I errors (Eklund et al., 2016), the overlap across two different TR acquisitions provides some evidence for the reliability of these effects. There was a positive quadratic effect for the thalamus in the slow TR group and a negative quadratic effect for the right lateral ventral temporal cortex in both TR groups. The positive quadratic cluster corrected effect in the slow TR group did overlap with a positive quadratic effect in the fast TR group that was not cluster corrected (voxel-wise $p < 0.05$; **Figure 5**). This demonstrates that an area of the thalamus had high MSSD in young and old age but low MSSD in middle age. The positive quadratic overlapping TR group effect was in a more dorsal-anterior portion of the thalamus compared to the linear MSSD decrease effect that was in a more ventral posterior portion of the thalamus. The negative quadratic effect in both groups was in the right lateral ventral temporal cortex (**Figure 5**). This demonstrates that an area in the right ventral temporal cortex had low MSSD in young and old age but high MSSD in middle age.

Post-hoc Analysis of Gray Matter Probability, Gender, Linear, and Quadratic Effects

To examine the specificity of the voxel-wise effects, we performed three follow-up post-hoc tests to examine whether these relationships could be accounted for by age-related changes in GMP or gender and to further explore linear and quadratic effects. The first post-hoc regression model used linear age, handedness, IQ, FD, gray matter probability, and gender. This test produced significant post-hoc effects for linear age for all overlapping ROIs across both TRs except for the sensorimotor ROI in the slow TR group, which produced a marginally significant effect (**Table 1**). This demonstrates that significant linear effects persisted across the lifespan after accounting for gray matter probability and gender in the absence of a quadratic regressor.

The second post-hoc regression model added quadratic age as a factor of interest back into to the first post-hoc regression model and produced a significant positive quadratic effect for the ventral temporal cortex in the slow TR group, a marginally significant positive quadratic effect of the basal ganglia in the fast TR group, a marginally significant positive quadratic effect for the sensorimotor ROI in the fast TR group, and marginally significant positive quadratic effects for the thalamus in both the fast TR and slow TR groups (**Table 1**). All other quadratic effects were not significant. This confirms that a model including a quadratic factor outperforms a model including the linear factor only for most linear effects (except for the VTC in the slow TR group) after accounting for gray matter and gender. This also demonstrates a U-shaped influence on the sensorimotor ROI for the fast TR group, and U-shaped influences on the thalamus for both TR groups.

The third post-hoc regression model showed that the positive voxel-wise quadratic effect in the thalamus remained significant in both the fast TR group and the slow TR group (**Table 1**). One outlier from the fast TR group and one outlier from the slow TR group were removed for the quadratic thalamus effect (SD > 4). The negative voxel-wise quadratic effect in the right ventral temporal cortex also remained significant in both the fast TR group and slow TR group. This demonstrates that voxel-wise quadratic effects still persist after accounting for gray matter probability and gender.

Linear relationship between MSSD values for subjects in both TR groups

In order to determine the consistency of MSSD values for subjects present in both TR groups, Spearman's rank-order correlations were calculated for MSSD values from the 177 subjects common to both TR groups for all post-hoc analyses. Significant positive correlations were present for all effects tested in a post-hoc manner (left VTC linear increase: *rho(175)* = 0.324, p = 0.000011; right dorsal anterior insula linear increase: *rho(175)* = 0.473, $p = 2.89 \times 10^{-11}$; sensorimotor linear decrease: *rho(175)* = 0.638, $p = 1.39 \times 10^{-21}$; visual linear decrease: *rho(175)* = 0.694, $p = 8.41 \times 10^{-27}$; thalamus linear decrease: *rho(175)* = 0.601, $p = 9.40 \times 10^{-19}$; basal ganglia linear decrease: *rho(175)* = 0.462, $p = 9.67 \times 10^{-11}$; thalamus positive quadratic for 175 subjects (2 outliers removed for SD > 4): *rho(173)* = 0.492, $p = 9.40 \times 10^{-12}$; right VTC negative quadratic: *rho(175)* = 0.484, $p = 4.74 \times 10^{-12}$). This demonstrates that MSSD values were similar in both the fast and slow TR analyses for each subject that was present in both TR groups.

Age-FD and Age-Sample Size Relationships

One possible concern with the current study is related to how the association between age and FD may impact measures of MSSD across the lifespan. In order to further investigate the relationship between age and head motion (e.g., FD), linear regression models were run using age (mean centered) and age squared (squared mean center age) as regressors in a step-wise model. In the fast TR group, we observed a positive quadratic relationship between age and FD ($F(2,188) = 3.99$, $p = 0.02$, $R^2 = 0.04$; $\beta_{linear} = 0.092$, $p = 0.209$; $\beta_{qaudratic} = 0.164$, $p = 0.025$) while the slow TR group we observerd a positive linear relationship between age and FD ($F(1, 185) = 25.22$, p =

0.000001, $R^2 = 0.12$; $\beta_{linear} = 0.0346$, $p = 0.000001$). Adding a quadratic term to the linear model for the slow TR group failed to produce a significant change in the F statistic ($F_{change} = 0.756$). Scatterplots visualizing the age-FD relationship for both TR groups can be found at the bottom of Figure 1. Despite the significant relationships between age and FD, the voxel-wise and post-hoc regression analyses used FD as a nuisance regressor that accounted for such relationships while still demonstrating significant effects across both analyses.

Another possible concern related to the current study could be that there was an unequal age distribution of participants: this dataset includes more subjects in early and old age compared with middle age. In order to investigate if this unequal distribution led to over-fitting for young and older individuals compared with middle age individuals, we examined whether there was a relationship between age and the unstandardized residuals for each post-hoc regression analysis. Visual inspection of these scatterplots demonstrated that residuals were evenly distributed across the entire age range, suggesting that analysis did not systematically over-fit the regression line at young and old age.

Discussion

Brain signal variability has been linked to optimal neural function (Garrett et al., 2013) and has been hypothesized to help facilitate shifts between integrative and segregative brain networks (Tognoli and Kelso, 2014). Previous studies have focused on identifying differences in BOLD variability between younger and older adults within the context of task-based fMRI paradigms (Garrett et al., 2010, 2011, 2012). The current study examines resting-state BOLD variability across the lifespan for the first time. We find linear and quadratic changes in lifespan BOLD variability trajectories in distinct brain areas similar to lifespan changes in resting-state functional connectivity (Betzel et al., 2014) and task-related univariate activity (Kennedy et al., 2015). The current study also complements research demonstrating developmental maturation of structural brain properties such as total cerebral volume, and white/gray matter maturation (Giedd et al., 1999).

Overall, we find that variability increases linearly in SN nodes (anterior insula) and the VTC across the lifespan. In contrast, brain signal variability decreases across the lifespan in most every other brain area including subcortical, visual, sensorimotor, default mode, and central executive regions. Cluster corrected results across two TRs demonstrated BOLD signal variability linearly increased across age in the right dAI and left VTC, whereas linear decreases were localized bilaterally in visual, sensorimotor, thalamic, and basal ganglia areas. Lastly, we demonstrate preliminary support for a positive quadratic thalamus effect that was spatially distinct from the linear decrease thalamus effect, and a negative right VTC quadratic effect.

Brain Variability across the Lifespan

The current results align with research demonstrating that BOLD variability mostly decreases in old age; less brain regions show increased variability with old age (Garrett et al., 2010, 2011). However, the current results do not align with previous evidence for a general cortical-subcortical dichotomy, where subcortical areas increase in variability across age compared with cortical areas (Garrett et al., 2013). Instead, the current study found different MSSD trajectories based on functional systems (e.g., SN vs. the rest of the brain) rather than a subcortical-cortical dichotomy. These data also conflict with previous results showing both increases and decreases in BOLD variability across age in frontal, temporal, and parietal areas (Garrett et al., 2010; Garrett et al., 2013). The current study also conflicts with previous EEG results (McIntosh et al., 2008) and BOLD variability studies (Garrett et al., 2011) that led researchers to propose an inverted U-shaped trajectory where brain variability is low in children and older adults, but high in middle-age (Garrett et al., 2013).

One explanation for the divergent findings is that we used resting state data, whereas previous studies focused on fixation and task-periods within the context of task performance. Previous research indicates that completing task-based fMRI affects resting state BOLD fMRI (Northoff et al., 2010). Thus, preceding task trials in task-based fMRI may affect variability analyzed during fixation periods. Furthermore, it is typical to isolate low frequency fluctuations in resting state data through bandpass filtering (0.01 – 0.10 Hz), something typically not done in task-based fMRI BOLD variability analyses. Finally, the current study used multi-band acquisition data whereas previous studies did not. Additional research should explore how interspersed task blocks affect BOLD variability during fixation periods compared to rest, how BOLD variability may differ when isolating specific frequency bands, and the influence of multi-band acquisition parameters on BOLD variability.

Functional Connectivity across the Lifespan

Two previous studies using the NKI-database (7-85 years old, TR = 2.5) demonstrate that modularity (how well major networks are partitioned into smaller integrative and segregative communities [e.g., SN, DMN]) generally shows a linear decrease across the lifespan, indicating reduced functional sub-network autonomy (Betzel et al., 2014; Cao et al., 2014). Betzel et al., (2014) also demonstrated general within-network node functional connectivity decreases alongside general between-network node functional connectivity increases for the DMN, CEN, visual, and sensorimotor networks. In the current study, general decreases in MSSD across the lifespan for most networks (except the SN) may be related to decreased modularity as increased variability is thought to enhance functional specificity by facilitating flexibly switching between integrative and segregative states (Tognoli and Kelso, 2014).

Additionally, Betzel et al. (2014) found that salience/ventral attention network nodes (including the right dAI) demonstrated positive quadratic trajectories for within-network node comparisons. They also found increased lifespan between-node connectivity involving the dorsal attention network, DMN, and CEN. Thus, the dAI demonstrated functional connections in different directions from the general decreased connectivity found between most other brain areas. Cao et al. (2014) conducted ROI-to-whole-brain functional connectivity analyses and demonstrated linear decreases of whole-brain functional connectivity metrics for nodes within salience (including the right dAI), default, attention, visual, and subcortical regions; positive quadratic effects were found for the parahippocampus and thalamus while negative quadratic effects were found in frontal, temporal, and parietal areas.

The current results demonstrating differential variability patterns in the right dAI compared with other brain areas are in accord with Betzel et al., where the right dAI showed differential patterns of functional connectivity across the lifespan compared with the rest of the cortex. The positive thalamic quadratic effect and the negative quadratic effect for the VTC in the current study align with Cao et al., who found a positive thalamic quadratic effect and negative temporal quadratic effect for functional connectivity. Other work indicates that dorsal-anterior portions of the thalamus strengthen their functional connections to frontal areas while ventral-posterior portions of the thalamus weaken their functional connections to temporal areas from childhood to adulthood (Fair et al., 2010). These dissociations in thalamic connectivity mirror the spatially distinct thalamic variability results in the current study where a dorsal-anterior thalamic area demonstrates a positive quadratic effect and a ventral-posterior thalamic area demonstrates a negative linear effect. These studies, in conjunction with the current study, suggest that the right dAI, thalamus, and temporal cortex present with unique types of variability and functional connectivity lifespan trajectories compared to other brain areas. Future work is needed to explore the relationship between BOLD variability and functional connectivity across the lifespan.

Behavioral Relevance of MSSD Lifespan Trajectories

On a systems level, different brain networks interacting with varying degrees of variability may reflect the inverted *u*-curve trajectories (**Figure 6**) for various behavioral measures (Cepeda et al., 2001; Hommel et al., 2004; Li et al., 2004; De Luca and Leventer, 2008; Tran and Formann, 2008). The right dAI within the SN in particular has been identified as a "hub" that participates in a myriad of cognitive processes including network switching, salience detection (Menon and Uddin, 2010), and integrating sensory networks (Nomi et al., 2016). Thus, increased variability in the right dAI is notable because of its dynamic interaction with almost every brain system and its involvement in nearly every cognitive process (Uddin, 2015). Speculatively, it is possible that large differences in variability between SN nodes and other brain areas/systems could produce the sub-optimal behavioral performance seen in early childhood and old age. In middle-age, variability between different brain areas/systems may reach more of an equilibrium, resulting in optimal behavioral performance - an idea consistent with theories proposing a balance between excitation and inhibitory neuronal processes facilitates optimal brain function (Shew et al., 2011). Additional studies that characterize the relationship between resting-state and task-based fMRI BOLD variability across the lifespan are crucial for understanding the behavioral significance of the current findings.

Physiological Influences on the BOLD Signal across the Lifespan

A concern in lifespan neuroimaging studies is neuro-vascular coupling – i.e., how neural activity interacts with brain vasculature across age to artificially influence the BOLD signal (D'Esposito et al., 2003). Although it is difficult to completely rule out physiological confounds, previous work suggests that vascular changes are not responsible for the BOLD variability trajectories observed in the current study. First, previous developmental BOLD variability research argued that global uni-directional vascular-coupling age effects cannot explain multi-directional BOLD variability trajectories (Garrett et al., 2010). Second, while early studies demonstrated an influence of vascular coupling on BOLD signal activity in aging research (D'Esposito et al., 1999), recent studies claim that these effects were driven by the inclusion of voxels biased towards younger subjects' task-activation in statistical analyses (Aizenstein et al., 2004) and by using task-designs that produce attentional and motor differences in older individuals compared with younger individuals (Grinband et al., 2017). Because the current study found multi-directional trajectories of BOLD variability (increases, decreases, and quadratic effects), avoided analyzing voxels biased towards any age range by focusing analyses on only voxels with significant age trajectories, and used resting-state fMRI data that were not influenced by task design, vascular coupling influences across age should be minimized.

Summary

The current study identified general lifespan trajectories of resting-state BOLD variability that complements previous research showing structural and functional lifespan changes within the brain. We demonstrate that variability in SN nodes increase linearly across the lifespan, whereas variability from most other large-scale networks decreases linearly over the lifespan. We also demonstrate positive quadratic thalamic effect and a negative quadratic right VTC effect. These findings add to a growing literature demonstrating the contributions of neural variability to flexible cognition.

References

Aizenstein HJ, Clark KA, Butters MA, Cochran J, Stenger VA, Meltzer CC, Reynolds CF, Carter CS (2004) The BOLD hemodynamic response in healthy aging. Journal of cognitive neuroscience 16:786-793.

Arbabshirani MR, Damaraju E, Phlypo R, Plis S, Allen E, Ma S, Mathalon D, Preda A, Vaidya JG, Adali T (2014) Impact of autocorrelation on functional connectivity. NeuroImage 102:294-308.

Armbruster-Genç DJ, Ueltzhöffer K, Fiebach CJ (2016) Brain Signal Variability Differentially Affects Cognitive Flexibility and Cognitive Stability. The Journal of Neuroscience 36:3978-3987.

Beck JM, Ma WJ, Kiani R, Hanks T, Churchland AK, Roitman J, Shadlen MN, Latham PE, Pouget A (2008) Probabilistic population codes for Bayesian decision making. Neuron 60:1142-1152.

Betzel RF, Byrge L, He Y, Goñi J, Zuo X-N, Sporns O (2014) Changes in structural and functional connectivity among resting-state networks across the human lifespan. NeuroImage 102:345-357.

Cao M, Wang J-H, Dai Z-J, Cao X-Y, Jiang L-L, Fan F-M, Song X-W, Xia M-R, Shu N, Dong Q (2014) Topological organization of the human brain functional connectome across the lifespan. Developmental cognitive neuroscience 7:76-93.

Cepeda NJ, Kramer AF, Gonzalez de Sather J (2001) Changes in executive control across the life span: examination of task-switching performance. Developmental psychology 37:715.

Craig AB (2009) How do you feel--now? The anterior insula and human awareness. Nature Reviews Neuroscience:59-70.

D'Esposito M, Deouell LY, Gazzaley A (2003) Alterations in the BOLD fMRI signal with ageing and disease: a challenge for neuroimaging. Nature Reviews Neuroscience 4:863-872.

D'Esposito M, Zarahn E, Aguirre GK, Rypma B (1999) The effect of normal aging on the coupling of neural activity to the bold hemodynamic response. NeuroImage 10:6-14.

Damoiseaux JS, Rombouts SA, Barkhof F, Scheltens P, Stam CJ, Smith SM, Beckmann CF (2006) Consistent resting-state networks across healthy subjects. Proceedings of the National Academy of Sciences of the United States of America 103:13848-13853.

Damoiseaux JS, Beckmann CF, Arigita EJ, Barkhof F, Scheltens P, Stam CJ, Smith SM, Rombouts SA (2008) Reduced resting-state brain activity in the "default network" in normal aging. Cerebral cortex 18:1856-1864.

De Luca CR, Leventer RJ (2008) Developmental trajectories of executive functions across the lifespan. Executive functions and the frontal lobes: A lifespan perspective 3:21.

Eklund A, Nichols TE, Knutsson H (2016) Cluster failure: Why fMRI inferences for spatial extent have inflated false-positive rates. Proceedings of the National Academy of Sciences:201602413.

Fair D, Bathula D, Mills K, Costa Dias T, Blythe M, Zhang D, Snyder A, Raichle M, Stevens A, Nigg J, Nagel B (2010) Maturing thalamocortical functional connectivity across development. Frontiers in systems neuroscience 4.

Garrett DD, Kovacevic N, McIntosh AR, Grady CL (2010) Blood oxygen level-dependent signal variability is more than just noise. The Journal of Neuroscience 30:4914-4921.

Garrett DD, Kovacevic N, McIntosh AR, Grady CL (2011) The importance of being variable. The Journal of Neuroscience 31:4496-4503.

Garrett DD, Kovacevic N, McIntosh AR, Grady CL (2012) The modulation of BOLD variability between cognitive states varies by age and processing speed. Cerebral cortex:bhs055.

Garrett DD, Samanez-Larkin GR, MacDonald SW, Lindenberger U, McIntosh AR, Grady CL (2013) Moment-to-moment brain signal variability: a next frontier in human brain mapping? Neuroscience & Biobehavioral Reviews 37:610-624.

Giedd JN, Blumenthal J, Jeffries NO, Castellanos FX, Liu H, Zijdenbos A, Paus T, Evans AC, Rapoport JL (1999) Brain development during childhood and adolescence: a longitudinal MRI study. Nature neuroscience 2:861-863.

Griffanti L, Salimi-Khorshidi G, Beckmann CF, Auerbach EJ, Douaud G, Sexton CE, Zsoldos E, Ebmeier KP, Filippini N, Mackay CE (2014) ICA-based artefact removal and accelerated fMRI acquisition for improved resting state network imaging. NeuroImage 95:232-247.

Grinband J, Steffener J, Razlighi QR, Stern Y (2017) BOLD neurovascular coupling does not change significantly with normal aging. Human brain mapping:n/a-n/a.

Hommel B, Li KZ, Li S-C (2004) Visual search across the life span. Developmental psychology 40:545.

Kennedy KM, Rodrigue KM, Bischof GN, Hebrank AC, Reuter-Lorenz PA, Park DC (2015) Age trajectories of functional activation under conditions of low and high processing demands: an adult lifespan fMRI study of the aging brain. NeuroImage 104:21-34.

Li S-C, Lindenberger U, Hommel B, Aschersleben G, Prinz W, Baltes PB (2004) Transformations in the couplings among intellectual abilities and constituent cognitive processes across the life span. Psychological Science 15:155-163.

McIntosh AR, Kovacevic N, Itier RJ (2008) Increased brain signal variability accompanies lower behavioral variability in development. PLoS Comput Biol 4:e1000106.

McIntosh AR, Kovacevic N, Lippe S, Garrett D, Grady C, Jirsa V (2010) The development of a noisy brain. Archives italiennes de biologie 148:323-337.

Menon V, Uddin LQ (2010) Saliency, switching, attention and control: a network model of insula function. Brain Structure and Function 214:655-667.

Nomi JS, Farrant K, Damaraju E, Rachakonda S, Calhoun VD, Uddin LQ (2016) Dynamic functional network connectivity reveals unique and overlapping profiles of insula subdivisions. Human brain mapping 37:1770-1787.

Nooner KB et al. (2012) The NKI-Rockland Sample: A Model for Accelerating the Pace of Discovery Science in Psychiatry. Frontiers in neuroscience 6:152.

Northoff G, Qin P, Nakao T (2010) Rest-stimulus interaction in the brain: a review. Trends in neurosciences 33:277-284.

Oldfield RC (1971) The assessment and analysis of handedness: the Edinburgh inventory. Neuropsychologia 9:97-113.

Samanez-Larkin GR, Kuhnen CM, Yoo DJ, Knutson B (2010) Variability in nucleus accumbens activity mediates age-related suboptimal financial risk taking. The Journal of Neuroscience 30:1426-1434.

Shew WL, Yang H, Yu S, Roy R, Plenz D (2011) Information capacity and transmission are maximized in balanced cortical networks with neuronal avalanches. The Journal of neuroscience 31:55-63.

Smith SM et al. (2013) Resting-state fMRI in the Human Connectome Project. NeuroImage 80:144-168.

Tognoli E, Kelso JS (2014) The metastable brain. Neuron 81:35-48.

Tran US, Formann AK (2008) Piaget’s water-level tasks: performance across the lifespan with emphasis on the elderly. Personality and Individual Differences 45:232-237.

Uddin LQ (2015) Salience processing and insular cortical function and dysfunction. Nature reviews Neuroscience 16:55-61.

Uddin LQ, Kinnison J, Pessoa L, Anderson ML (2014) Beyond the tripartite cognition-emotion-interoception model of the human insular cortex. Journal of cognitive neuroscience 26:16-27.

Von Neumann J, Kent R, Bellinson H, Hart Bt (1941) The mean square successive difference. The Annals of Mathematical Statistics 12:153-162.

Table 1: Regression results from three post-hoc models. Model 1 examined if linear effects persisted across the lifespan in the absence of a quadratic regressor when averaging MSSD across a group of voxels and accounting for gray matter probability and gender. Model 2 ruled out that a quadratic effect better explained the linear effect from model 1 when averaging MSSD across a group of voxels and accounting for gray matter probability and gender. Model 3 examined if quadratic effects persisted across the lifespan when averaging MSSD across a group of voxels and accounting for gray matter probability and gender. VTC = ventral temporal cortex. Beta coefficients are reported in standardized form.

Figure 1: Age (top row) and gender distribution (middle row) in the fast and slow TR groups. Scatterplots for each TR group that represent the relationship between age and framewise displacement are pictured in the bottom row.

Figure 2: Liberal voxel-wise corrected ($p < 0.40$ uncorrected) *t*-maps without cluster correction. Blue represents the fast TR group while red represents the slow TR group. General linear MSSD increases can be seen in salience network nodes such as the bilateral anterior insula and anterior cingulate cortex, and also in the ventral temporal cortex. General linear MSSD decreases can be seen in subcortical, visual, sensorimotor, default mode (posterior cingulate and medial pre-frontal cortex), and central executive (supramarginal gyrus and dorsal-lateral pre-frontal cortex) brain areas. Colorbars represent t-values.

Figure 3: T-maps showing brain areas surviving voxel-wise ($p < 0.002$ uncorrected) and cluster size ($p < 0.05$ corrected) associations between MSSD and age. Red = slow TR group (1.4 secs), Blue = fast TR group (0.645 secs), Violet = voxel overlap between fast and slow TR groups, neuroscientific convention. Significant cluster-corrected voxels overlapping across both TR groups demonstrate linear increases in the right anterior cingulate and left ventral temporal cortex and linear decreases in thalamus, sensorimotor cortex, and in the primary visual cortex. Brain slices are the same as those in Figure 2.

Figure 4: Scatter plots depicting linear MSSD effects across the lifespan. ROIs were taken from areas of cluster-corrected TR group overlap (violet colors) in Figure 3. Blue circles = male, red circles = female.

Figure 5: Top: Spatially distinct voxels showing linear decrease and positive quadratic effects in the thalamus. Blue = voxels overlapping across both TR groups showing a linear MSSD decrease. Red = voxels overlapping across both TR groups for a positive quadratic MSSD effect. Scatter plots show MSSD values for the fast TR group effect (voxel-wise at $p < 0.05$) and slow TR group effect (voxel-wise at $p < 0.05$ and cluster corrected at $p < 0.05$). Bottom: Negative quadratic effect overlap for both TR groups with scatter plots showing MSSD effects (voxel-wise at $p < 0.05$ and cluster corrected at $p < 0.05$ for both TR groups). Blue circles = male, red circles = female.

Figure 6: Speculative model describing the proposed relationship between linear increases and decreases in BOLD variability across the lifespan and the inverted U-shaped curve of lifespan behavioral performance characterizing many behavioral tasks. The yellow arrow indicates linear increases in BOLD variability for salience network nodes, while the blue arrow indicates linear decreases in BOLD variability for central executive (CEN), default mode (DMN), sensorimotor (SM), and visual areas. In early- and old-age, large differences in variability between brain networks leads to sub-optimal behavioral performance. The red arrows indicate that optimal behavioral performance may come from the intrinsic balance between high and low variability between different brain networks in middle-age.

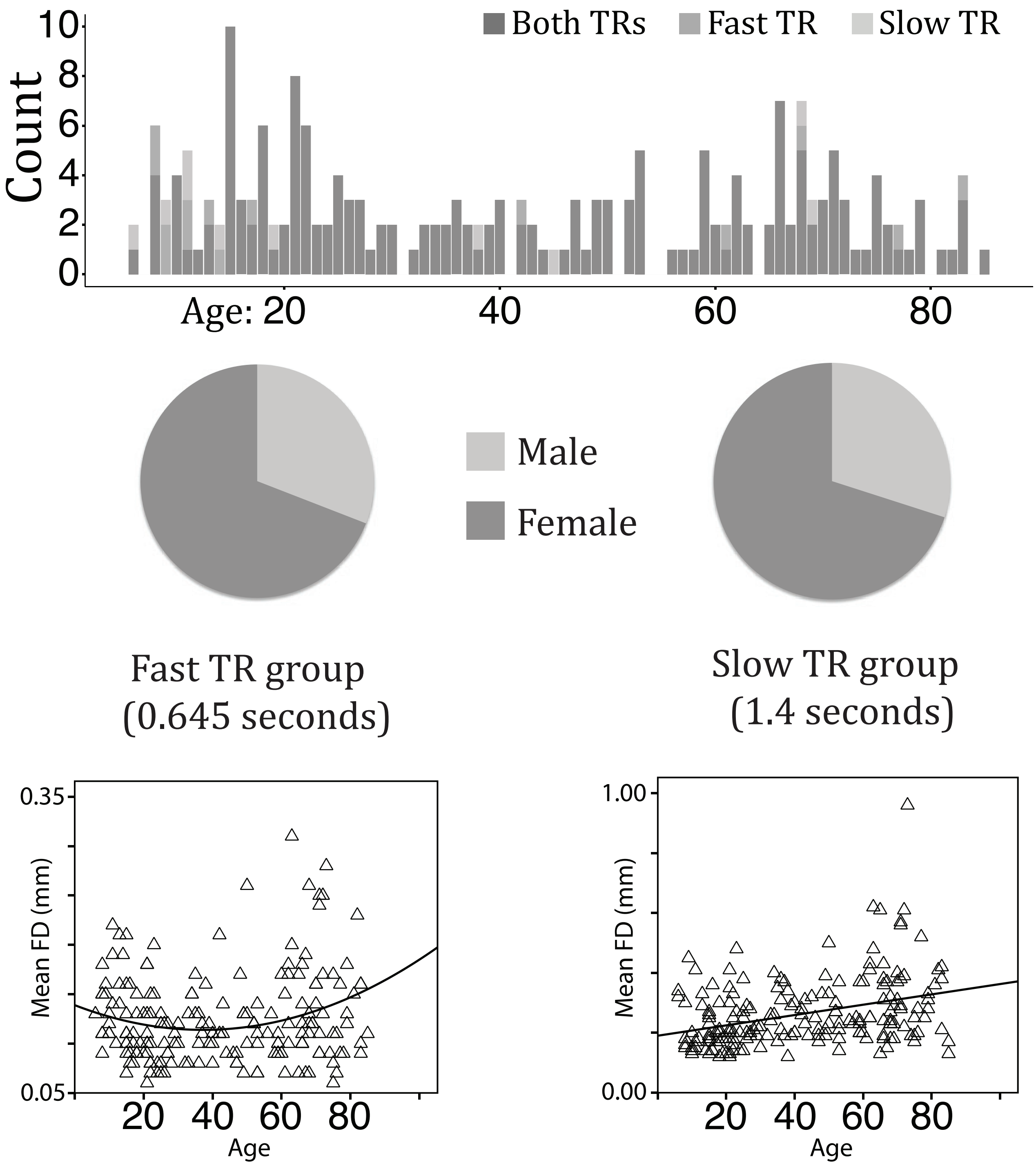
Both TRs
Fast TR
Slow TR
Count
Age: 20
40
60
80
Male
Female
Fast TR group
(0.645 seconds)
Slow TR group
(1.4 seconds)
Mean FD (mm)
0.35
0.05
1.00
0.00
Age

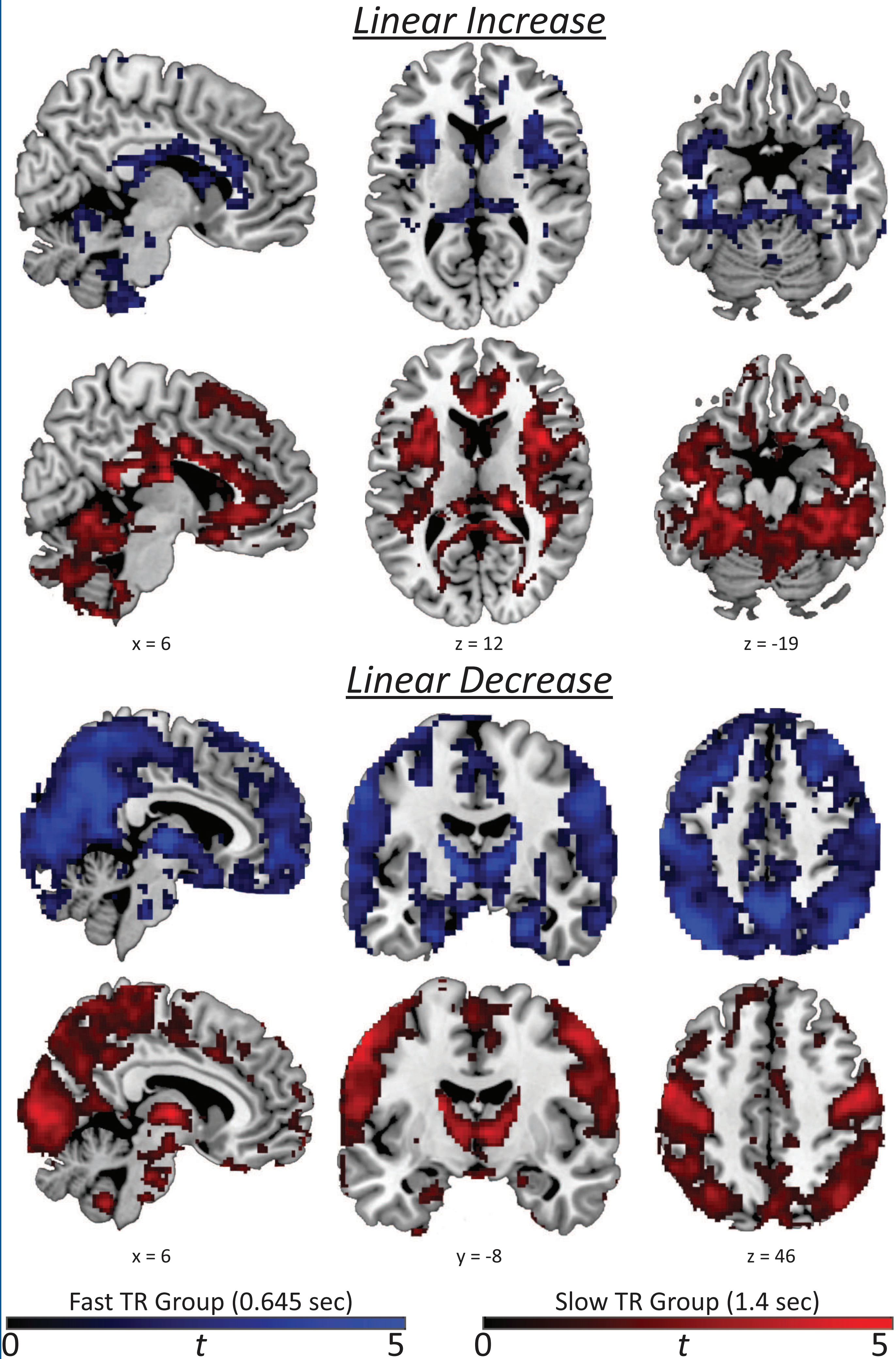
Linear Increase
x = 6
z = 12
z = -19
Linear Decrease
x = 6
y = -8
z = 46
Fast TR Group (0.645 sec)
0
t
5
Slow TR Group (1.4 sec)
0
t
5

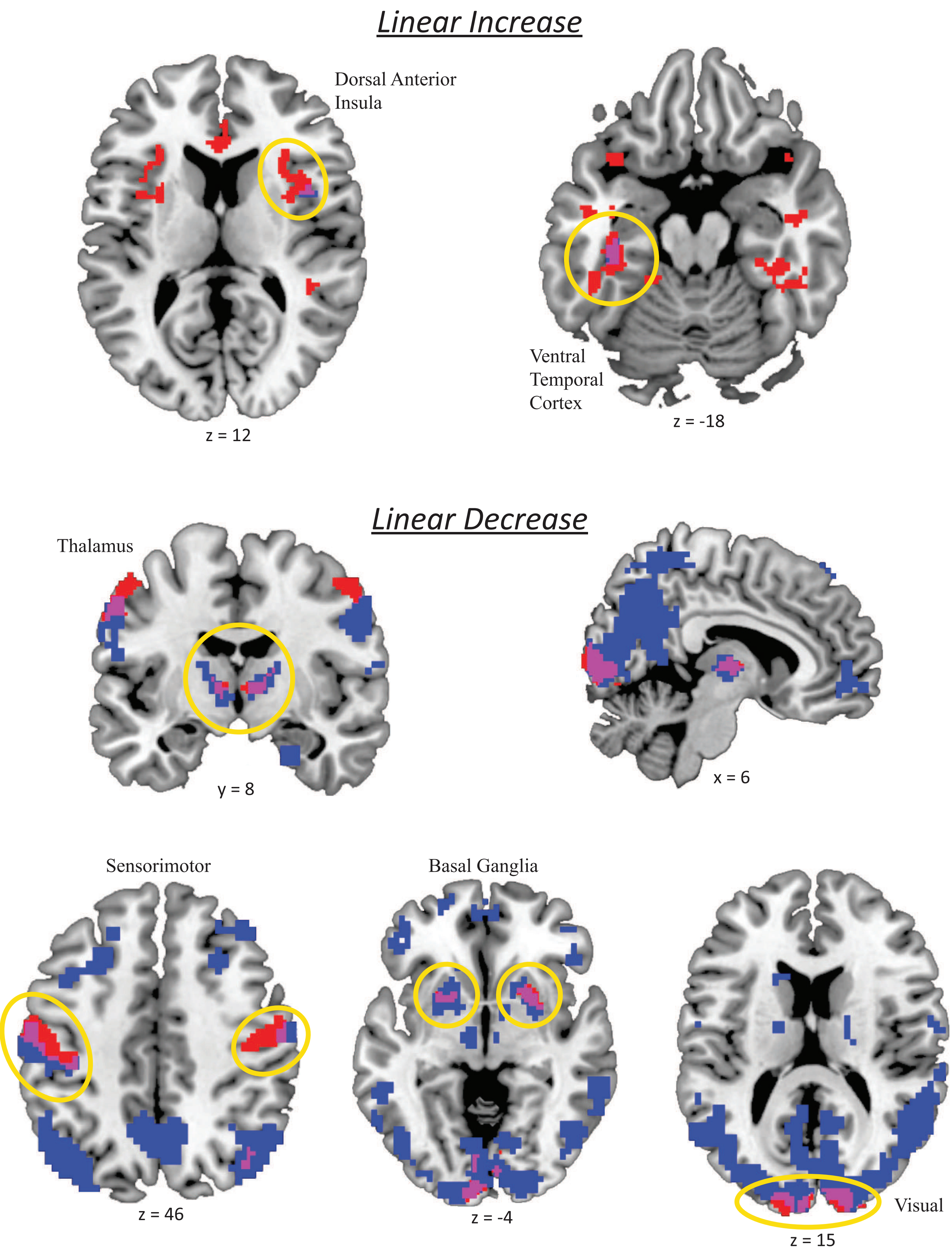
Linear Increase
Dorsal Anterior
Insula
z = 12
Ventral
Temporal
Cortex
z = -18
Linear Decrease
Thalamus
y = 8
x = 6
Sensorimotor
z = 46
Basal Ganglia
z = -4
Visual
z = 15

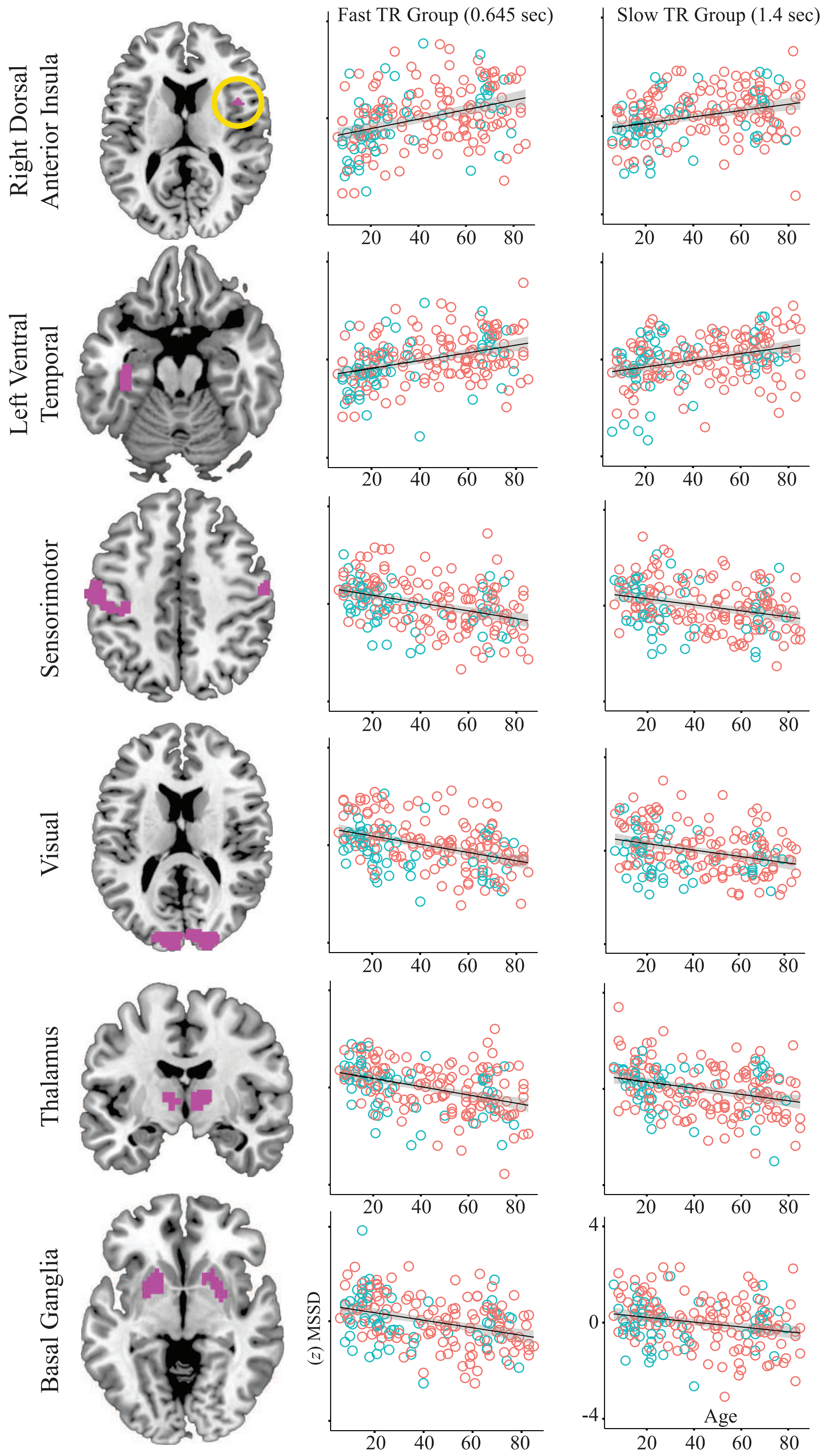

Fast TR Group (0.645 sec)
Slow TR Group (1.4 sec)
Right Dorsal Anterior Insula
Left Ventral Temporal
Sensorimotor
Visual
Thalamus
Basal Ganglia
(z) MSSD
Age
4
0
-4
20
40
60
80

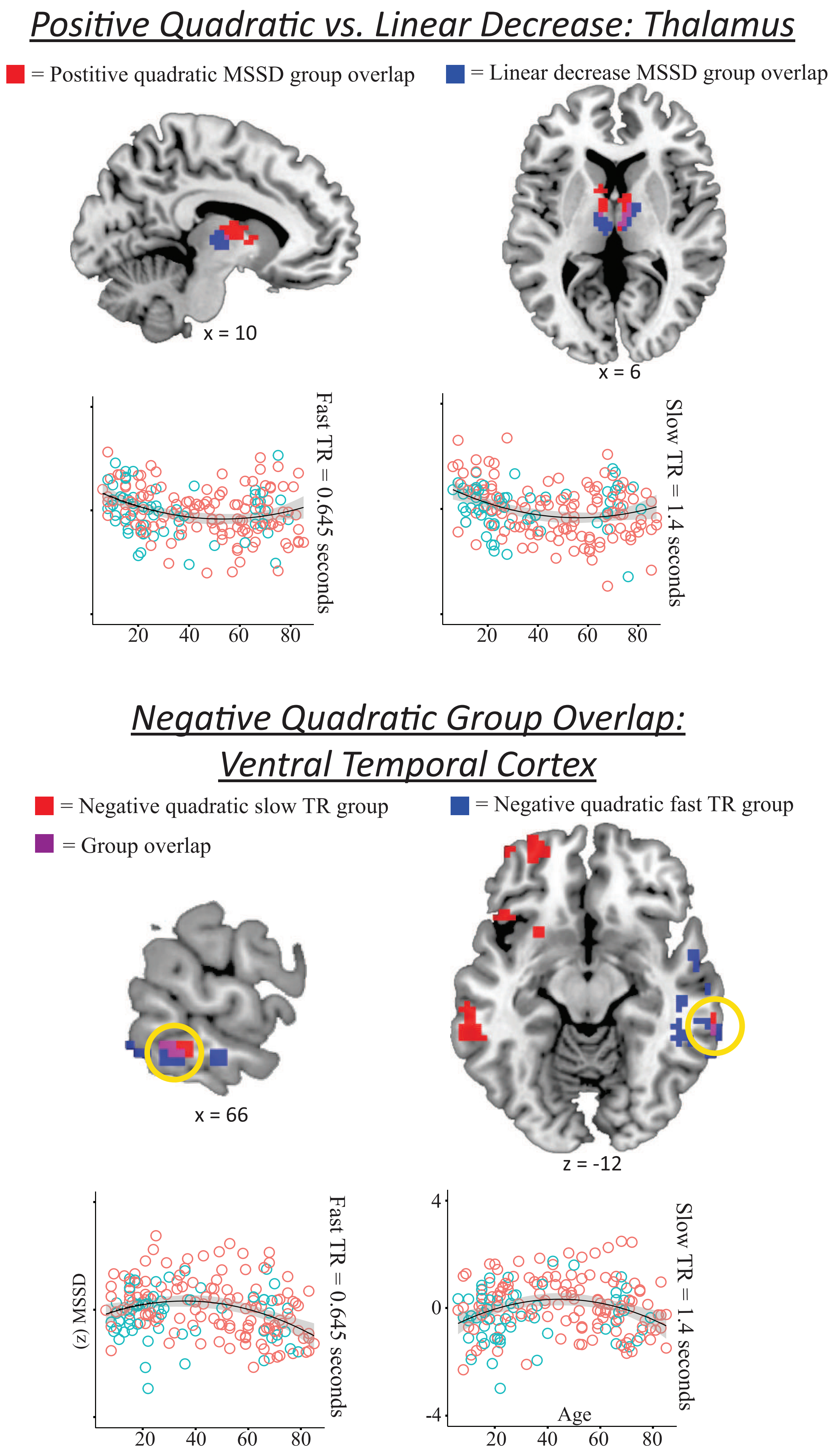
Positive Quadratic vs. Linear Decrease: Thalamus
= Postitive quadratic MSSD group overlap
= Linear decrease MSSD group overlap
x = 10
x = 6
Fast TR = 0.645 seconds
Slow TR = 1.4 seconds
20
40
60
80
Negative Quadratic Group Overlap:
Ventral Temporal Cortex
= Negative quadratic slow TR group
= Negative quadratic fast TR group
= Group overlap
x = 66
z = -12
(z) MSSD
4
0
-4
Age
Fast TR = 0.645 seconds
Slow TR = 1.4 seconds
20
40
60
80

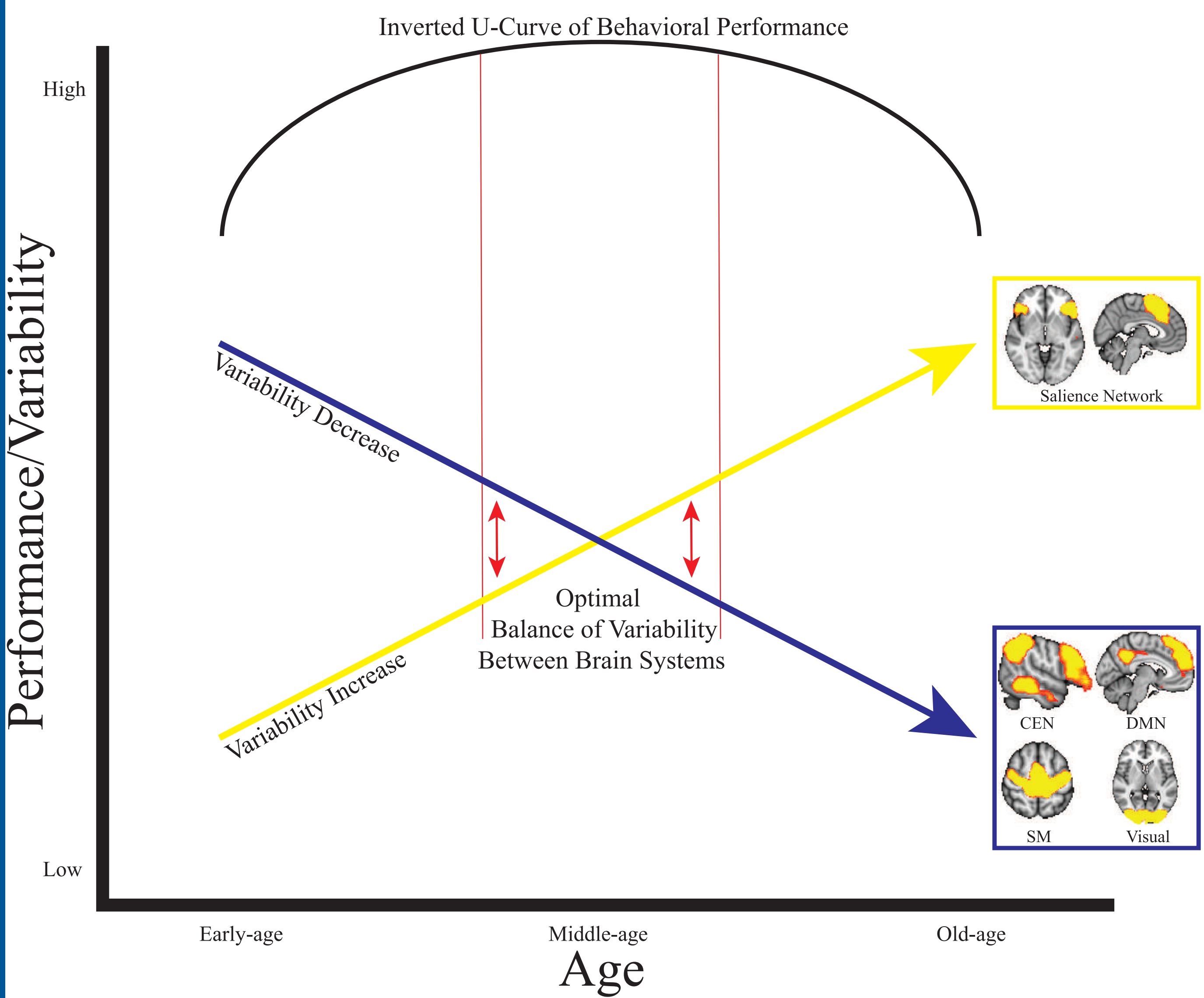
Inverted U-Curve of Behavioral Performance
High
Low
Performance/Variability
Variability Decrease
Variability Increase
Optimal
Balance of Variability
Between Brain Systems
Salience Network
CEN
DMN
SM
Visual
Early-age
Middle-age
Old-age
Age

Table 1: Results from post-hoc regression analyses.

		Fast TR group (0.645 seconds)				Slow TR group (1.4 seconds)				
		R^2	(*df*) F	β_{linear} (*p* value)	$\beta_{quadratic}$ (*p* value)		R^2	(*df*) F	β_{linear} (*p* value)	$\beta_{quadratic}$ (*p* value)
Left VTC Linear Increase	M1	0.188	(6, 184) 7.09	0.379 (4.8548×10^{-7})	-	M1	0.202	(6, 180) 7.61	0.349 (0.00001)	-
	M2	0.195	(7, 183) 6.32	0.394 (2.5402×10^{-7})	-0.090 (0.215)	M2	0.210	(7, 179) 6.81	0.361 (0.000005)	-0.097 (0.178)
Right Insula Linear Increase	M1	0.158	(6, 184) 5.78	0.283 (0.0006)	-	M1	0.122	(6, 180) 4.17	0.271 (0.0028)	-
	M2	0.159	(7, 183) 4.94	0.288 (0.0007)	-0.022 (0.771)	M2	0.150	(7, 179) 4.51	0.310 (0.00068)	-0.183 (0.016)
Sensorimotor Linear Decrease	M1	0.175	(6, 184) 6.49	-0.327 (0.004)	-	M1	0.132	(6, 180) 4.56	-0.210 (0.0776)	-
	M2	0.188	(7, 183) 6.06	-0.368 (0.0015)	0.126 (0.084)	M2	0.132	(7, 179) 3.89	-0.214 (0.0779)	0.012 (0.871)
Visual Linear Decrease	M1	0.211	(6, 184) 9.49	-0.424 (4.1261×10^{-7})	-	M1	0.171	(6, 180) 6.21	-0.383 (0.00002)	-
	M2	0.210	(7, 183) 8.23	-0.434 (3.005×10^{-7})	0.061 (0.382)	M2	0.176	(7, 179) 5.45	-0.393 (0.000015)	0.071 (0.333)
Thalamus Linear Decrease	M1	0.151	(6, 184) 6.61	-0.428 (3.2781×10^{-7})	-	M1	0.103	(6, 180) 3.44	-0.300 (0.00105)	-
	M2	0.162	(7, 183) 6.23	-0.424 (3.5265×10^{-7})	0.139 (0.065)	M2	0.119	(7, 179) 3.44	-0.297 (0.0011)	0.139 (0.075)
Basla Ganglia Linear Decrease	M1	0.110	(6, 184) 4.90	-0.409 (0.0004)	-	M1	0.084	(6, 180) 2.75	-0.216 (0.0117)	-
	M2	0.120	(7, 183) 4.71	-0.484 (0.0008)	0.140 (0.075)	M2	0.085	(7, 179) 2.37	-0.223 (0.0105)	0.037 (0.639)
Thalamus Postive Quadratic	M3	0.097	(6, 183) 3.26	-0.264 (0.00054)	0.206 (0.011)	M3	0.102	(6, 179) 3.38	-0.240 (0.003)	0.205 (0.008)
Right VTC Negative Quadratic	M3	0.184	(7, 183) 5.89	-0.202 (0.030)	-0.169 (0.021)	M3	0.111	(7, 179) 3.18	-0.095 (0.342)	-0.252 (0.0011)